Istraživanja i projektovanja za privredu
ISSN 1451-4117
DOI:10.5937/jaes0-45624
www.engineeringscience.rs

iipp publishing

Journal of Applied Engineering Science
Vol. 22, No. 4, 2024
Original Scientific Paper
Paper number: 22(2024)4, 1234, 707-717

ANALYZING THE EFFECTS OF MANUFACTURING PARAMETERS MODIFICATION ON FINAL SURFACE ROUGHNESS IN SELECTIVE LASER MELTING PARTS

M. P. Calvo Correa*, C. J. Cortés Rodriguéz

Universidad Nacional de Colombia, Department of Mechanical and Mechatronic Engineering, Bogotá, Colombia
** mpcalvoc@unal.edu.co*

Selective Laser Melting (SLM) is an additive manufacturing technique widely used today for producing metal components. This method enables the fabrication of geometrically complex parts while reducing costs and production time compared to traditional manufacturing techniques. However, a notable drawback of SLM is its tendency to produce high surface roughness and superficial defects such as balling, porosity, debris, and waviness. This study evaluates the effects of modifying two manufacturing parameters—scanning speed and laser power—on the final surface roughness. To achieve this, cylindrical specimens were fabricated using various combinations of these parameters, and the resulting surface roughness metrics (Sa, Sq, Ssk, Sku, Sdr, among others) were measured using an optical 3D surface roughness measurement instrument. A Taguchi L8 design was applied to analyse the influence of the manufacturing parameters on the measured roughness characteristics. This study investigates the influence of laser power and scanning speed on surfaces manufactured through Selective Laser Melting (SLM) and their effects on the previously described roughness parameters. The authors observed that the manufacturing parameters have varying impacts on the final surface roughness of components produced via SLM. Due to the inherent characteristics of the process, a specific combination of parameters that reduces roughness within a specimen's layer may increase roughness at the layer boundaries. These findings underscore the complex relationship between manufacturing parameters and surface roughness in SLM-produced parts, emphasizing the need for strategies, such as surface finishing post-treatments, to achieve the desired surface quality.

Keywords: surface roughness, scanning speed, laser power, Sa, selective laser melting

1 INTRODUCTION

The Selective Laser Melting (SLM) technique is an additive manufacturing (AM) method that enables the production of metal components directly from a 3D model [1, 2]. This technology has recently gained significant popularity in research and industry [3]. SLM reduces production time and costs compared to traditional manufacturing methods such as forging or machining [4, 5]. Additionally, it facilitates the fabrication of customized materials with complex geometries, making it highly applicable in industries like orthopedic implants and material science [6, 7, 8].

Despite its numerous advantages, the SLM process faces challenges due to its inherent characteristics. These include manufacturing defects, low dimensional accuracy, pores, cracks, and high surface roughness [9, 10, 11, 12, 13]. Such defects can lead to issues such as premature fatigue failure, increased friction, residual stresses, and the need for extensive post-processing, ultimately raising the cost of the final product [14, 15, 16, 17].

Properly selecting and adjusting manufacturing parameters in the SLM process is critical to minimizing these defects. Parameters such as scan speed, laser power, and laser scanning strategy are widely recognized in the literature as critical factors in reducing surface defects [18, 19, 20].

This article presents an experimental and statistical analysis to identify the optimal manufacturing parameters for reducing surface roughness and enhancing surface quality in cobalt-chromium alloy components produced via SLM. Furthermore, it explores how these parameters influence various surface roughness metrics.

2 SURFACE ROUGHNESS IN PIECES MANUFACTURED BY SELECTIVE LASER MELTING

Components manufactured using the Selective Laser Melting (SLM) technique typically exhibit a final surface roughness (Sa) ranging from 10 µm to 30 µm [21]. This high surface roughness poses significant challenges, particularly for applications where the components are in contact with other surfaces. Increased roughness elevates the friction coefficient, which can ultimately lead to premature failure of the component [22, 23].

SLM-manufactured components are widely used in producing metal orthopedic implants tailored to individual patients. However, implants with high surface roughness values are more prone to bacteria colonization, wear debris formation, residual stresses, cracks, and premature failure [24, 25].

The inherent characteristics of the SLM process directly impact the resulting surface roughness. As a layer-by-layer manufacturing method, the process involves melting a material layer with a laser to achieve the desired shape. Once the melted layer solidifies, a new layer of powder is deposited on top, and the laser melts this layer to build upon the previous one. This sequence is repeated until the entire component is complete [4, 26].

During the melting phase, a molten material pool forms, exhibiting temperature gradients between its surface and the bottom, where it contacts the substrate [27]. These temperature differences affect the pool's surface tension, causing droplets of varying sizes to detach. These droplets are then dispersed across the surface due to a phenomenon known as the Marangoni effect [28, 29].

The Marangoni effect inherent to the SLM process contributes to forming defects such as debris and balling. Additionally, the process can result in unmelted or over-melted sections of material, leading to cracks, pores, and waviness. These defects, debris, and balling significantly influence the final surface roughness [30, 31].

Several studies, including those by Maleki et al., Singla et al., and Sreekanth et al., have highlighted the importance of adjusting manufacturing parameters, such as scanning speed and laser power, to minimize defects and improve final surface roughness in the SLM process [32, 33, 34]. For instance, Babu et al. reported that increasing laser power can reduce balling defects, whereas Elsayed et al. observed that higher scanning speeds can decrease final surface roughness [13, 35, 36].

3 METHODS AND MATERIALS

3.1 Materials

The Selective Laser Melting equipment used in this study was an MYSINT 100 from Sisma® [37]. The components manufactured were cylindrical, with 10 mm x 7 mm dimensions. The material employed was cobalt-chromium alloy, type Starbond Easy Powder 30®; this material has a grain size range of +10/-30 µm and is designed explicitly for SLM applications [37].

Table 1 presents the manufacturing parameters that remained constant throughout the experiment.

Fig 1 illustrates the dimensions, shape, and build direction of the specimens used in the experiment.

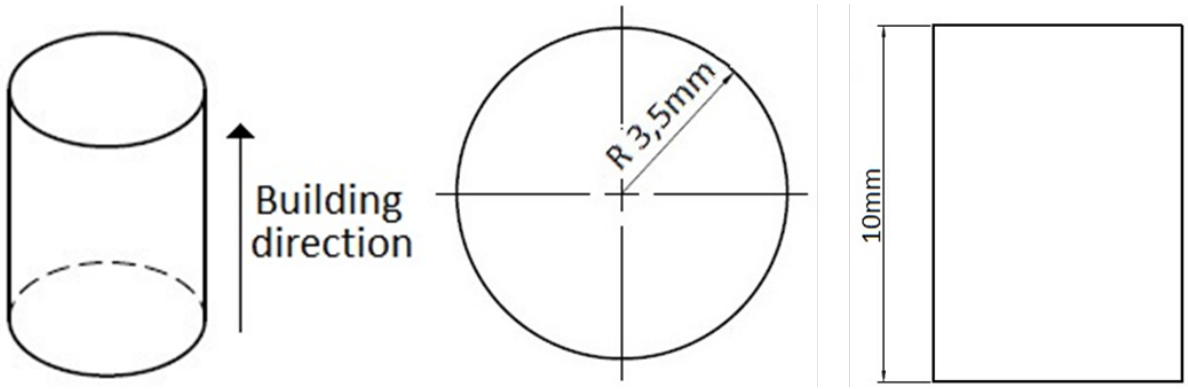

Fig. 1. Dimensions, shape, and build direction of the specimens used in the experiment

Table 1. Manufacture parameters kept constant during the experiment

Parameter	Value
Hatch laser	50 µm
Layer thickness	30 µm
Air speed	3 m/s
Number of layers	538
Oxygen level	50 %
Material used	CoCr (Starbond Easy Power 30)
Grain size	+10/-30 µm

Surface roughness was measured using an optical 3D measurement instrument, the Alicona Infinite Focus G5, part of the Precision Dimensional Metrology Laboratory at the Universidad Nacional [38]. This equipment utilizes Focus-Variation technology and is capable of measuring surface roughness in the µm and sub-µm range [39]. The measurement area was 9667.05 µm in width by 1624.33 µm in height. On average, 8,166,115 elements were analyzed using a cut-off wavelength (λc) of 8000.00 µm, according to ISO 16610-71, linear planar, order 2.

3.2 Methods

This study employed a fractional Taguchi L8 design, which was generated using Minitab Statistical Software® with the DOE-Taguchi tool [40].

For this experiment, two factors were varied: scanning speed and laser power. The levels for each factor were selected based on the literature and the equipment's allowable limits.

Table 3 presents the factors, their levels, and the corresponding combination values used in this investigation.

Table 2. Combination of parameters used. Source: Authors

Scan speed [mm/s]	Laser power [W]
500	75
500	125
600	75
600	125
700	75
700	125
800	75
800	125

The roughness for each combination of manufacturing parameters was measured in two different regions of the piece: the base of the cylinder and the side of the cylinder, with five repetitions per measurement.

The optimal set of manufacturing parameters was selected using the "smaller-the-better" criterion, with a significance level of 95%. The roughness measurement had an uncertainty of 0.04 µm.

3.3 Roughness parameters measured.

For this research were measured three different roughness parameters, each serving a specific purpose in metrology. The surface parameters measured were as follows:

- Sa- Arithmetic mean height: This parameter is widely used in surface engineering investigations. It represents the arithmetic mean of the absolute value of the height of the sampling area. However, Sa alone may not adequately describe the surface topography since different surfaces with varying peaks and valleys can yield the same Sa value. To provide a more comprehensive understanding of surface smoothness, it is recommended to report Sa alongside additional parameters such as Sz or Sdr [41, 42].
- Sq-Root means square height: This parameter, among Sa, are the more frequently parameters used for describing a surface. But as well as Sa, this parameter fails in describing the differences present between the peaks and valleys, and between different surface textures.
- Sz- Maximum surface height: This is the addition of the maximum height of the highest peak and the deepest valley [42].
- Sdr- Developed interfacial area radio: This parameter quantifies the percentage of the additional surface area contributed by texture compared to the planar definition area. When Sdr equals zero, it indicates an ideally flat surface [42, 43].
- Ssk- Skewness: This parameter quantifies the degree of skewness in the roughness profile, describing the surface's asymmetry. A Ssk equal to zero describes a surface with symmetric distribution of peaks and valleys around a median plane.
- Sku- Kurtosis: this parameter describes the nature of the surface. A Sku higher than 0 indicates a surface with mainly high peaks, and a Sku lower than 3 describes a surface with predominantly valleys.
- Vmc (p,q)- Core material volume: this volume parameter indicates the texture between the peaks and the valleys. This parameter is useful for tribological applications [42, 43].

4 RESULTS AND DISCUSSION.

Table 4 shows the roughness results obtained at the base of the cylinder. Table 5 presents the roughness results obtained for the side of the specimens.

Table 3. Roughness values obtained from the different combinations of manufacturing parameters.

Scanning speed [m/min]	Laser power [W]	Sa [µm]	Sq [µm]	Sz [µm]	Sku	Ssk	Sdr [%]	Vmc [ml/m^2]
30	75	45.6	57.4	395.5	2.9	0.36	31.0	51.2
30	125	22.8	28.6	272.2	3.3	0.08	7.5	26.3
36	75	36.9	47.5	518.1	4.3	0.6	49.1	40.3
36	125	21.8	27.3	229.2	2.9	0.23	7.5	24.9
42	75	24.4	32.3	361.9	6.2	0.83	39.0	26.4
42	125	13.6	17.4	195.8	3.70	0.08	8.7	14.9
48	75	16.0	20.7	571.6	10.0	-0.03	32.6	17.8
48	125	22.2	27.9	206.6	3.2	0.33	9.8	24.8

Table 4. Roughness surface parameters obtained for the side of the specimens. Source: Authors

Scanning speed [m/min]	Laser power [W]	Sa [µm]	Sq [µm]	Sz [µm]	Sku	Ssk	Sdr [%]	Vmc [ml/m2]
30	75	6.4	8.8	112.3	9.9	1.8	44.4	6.4

Scanning speed [m/min]	Laser power [W]	Sa [µm]	Sq [µm]	Sz [µm]	Sku	Ssk	Sdr [%]	Vmc [ml/m2]
30	125	4.0	5.3	69.0	6.8	1.0	11.2	4.3
36	75	8.9	12.9	207.3	12.4	2.2	78.5	8.4
36	125	7.8	10.3	167.3	5.3	0.7	28.8	8.5
42	75	9.8	13.1	152.2	6.0	1.4	85.0	9.9
42	125	10.2	13.5	115.9	5.2	1.2	93.3	10.3
48	75	10.1	13.6	158.9	6.3	1.4	87.2	10.2
48	125	9.1	11.7	116.1	3.9	0.5	46.3	10.14

4.1 Analysis of results

After conducting the statistical analysis, it was concluded that the manufacturing parameters have different effects on surface roughness for the Sa and Sq variables, depending on the measured specimen area. For these parameters, it was observed that the scanning speed affects the Sa parameter differently depending on the direction of the manufacturing process. To reduce the surface roughness (Sa) at the base of the cylinder, the scanning speed needs to be decreased; however, this adjustment leads to an increase in the Sa value on the top surface of the cylinder. This same trend was also observed for the Sq parameter.

Fig 2 illustrates the behavior of surface roughness (Sa) based on different manufacturing parameters. For the base of the specimens, increasing the scanning speed reduces surface roughness (Sa), while increasing the scanning speed on the sides of the specimens increases the Sa value.

Regarding the effect of laser power on surface roughness, the trend is consistent across different areas of the specimens: increasing the laser power decreases surface roughness (Sa). However, the impact of laser power on surface roughness is greater at the base than on the sides of the specimen.

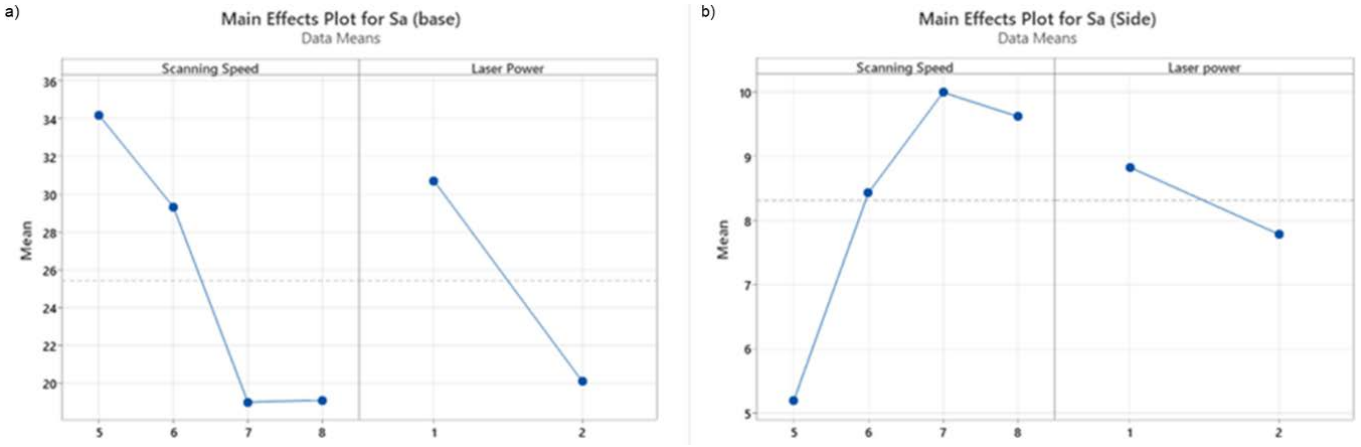

Fig. 2. Main effects plot for Sa across different areas of the specimens: (a) base, (b) side

The same behavior was observed for the surface roughness parameters Sq and Sz, with the manufacturing parameters exhibiting the same trends.

On the other hand, the surface roughness parameters Sku, Ssk, and Sdr did not follow the same trends concerning the manufacturing parameters. For the Sku parameter, the manufacturing parameter with the most significant effect was the scanning speed. In contrast, the most significant factor for the surface parameters Ssk and Sdr was the laser power. Similarly, it was observed that the effect of scanning speed depends on the manufacturing direction and the area being measured.

It is also worth noting that Sku and Ssk should be measured together to accurately describe the surface, as the combination of these two parameters can effectively characterize the surface. However, the statistical analysis revealed that no combination of parameters resulted in a symmetric distribution of peaks and valleys on the surface. The analysis of variance conducted for Sa and Vmc did not provide significant evidence that any of the selected manufacturing parameters had a substantial impact on the surface roughness response. In contrast, for the Sz and Sdr parameters, only the laser power parameter significantly influenced the surface roughness. These findings suggest that the selected manufacturing parameters have varying effects on different surface roughness parameters.

On the other hand, for the surface roughness parameter Sdr, it was found that laser power had the most significant influence on the final surface roughness. Interestingly, each manufacturing parameter affected Sdr differently depending on the area measured. For the base of the specimen, laser power had the most significant impact, with an increase in laser power resulting in a flatter surface. However, on the sides of the specimens, achieving the same effect required an increase in scanning speed.

Fig 3 shows the plot of the main effects of the manufacturing parameters on the Sdr results. Although the general trend of each manufacturing parameter is consistent across the entire specimen, the surface roughness parameter Sdr in each area is influenced by different manufacturing parameters.

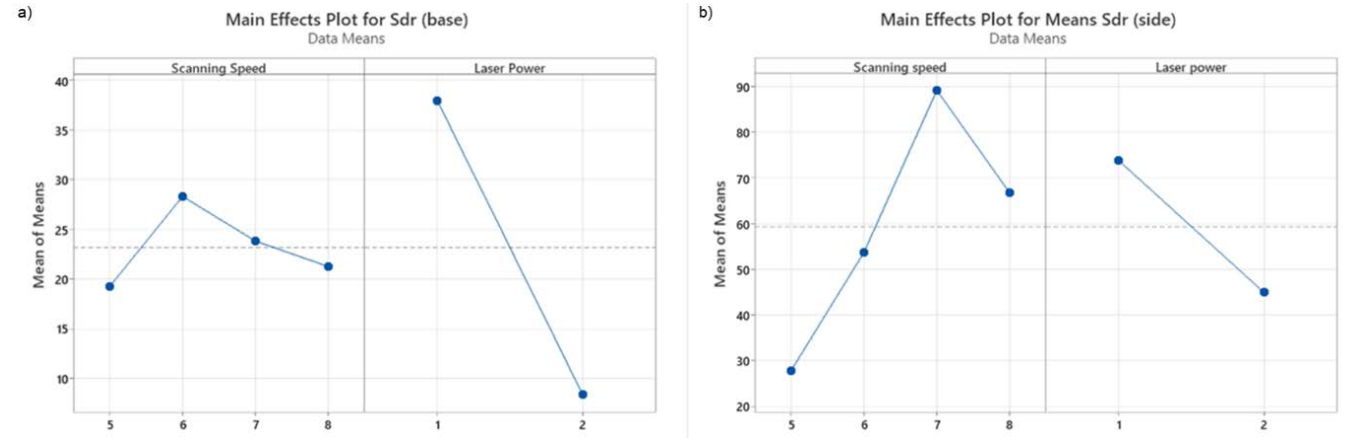

Fig. 3. Mean effects plot for the Sdr roughness parameter: (a) base, (b) side

Regarding the roughness parameters Svk, Spk, and Vcm, it is concluded that manufacturing parameters, laser power, and scanning speed significantly influence these parameters. Nevertheless, the behavior of these roughness values is similar to the roughness parameters evaluated previously. Depending on the area evaluated, the influence of laser power and scanning speed has a different effect on the surface roughness parameters Svk, Spk, and Vcm. In this case, it can be observed that increasing the scanning speed decreases the value of the roughness parameters on the sides but, at the same time, increases the value of these roughness parameters on the base of the specimens.

Fig 4 shows the mean effect plot for the roughness parameter Vmc. In this plot, it can be seen that the influence of laser power on the specimen affects the entire tested area uniformly. On the other hand, the scanning speed affects the side and the base of the specimen in opposite ways. On the base of the specimen, increasing the scanning speed increases the surface roughness (Vmc), while at the same time, this increase in scanning speed decreases Vmc on the sides of the specimens.

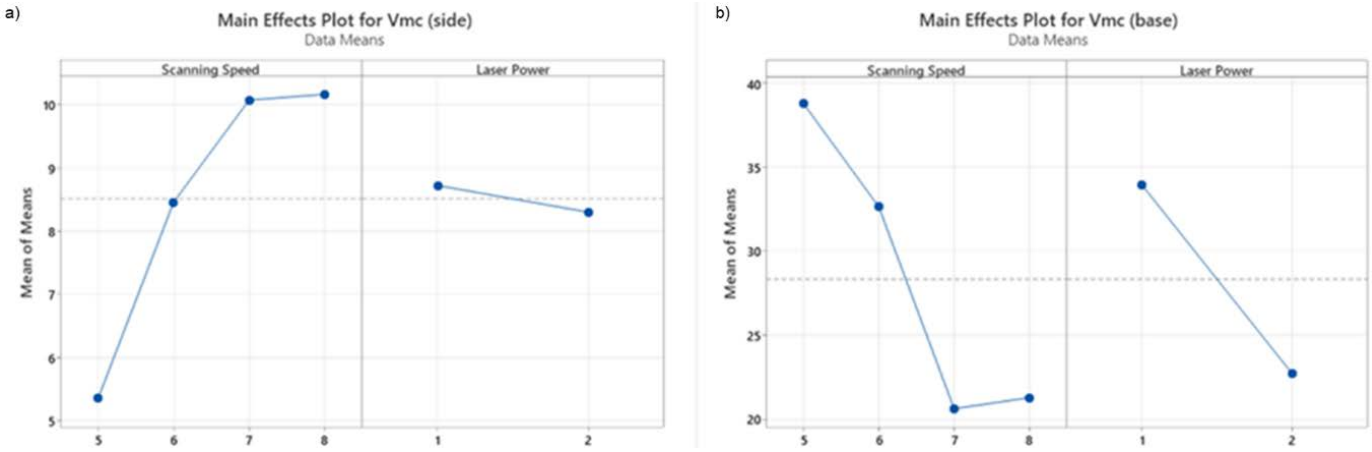

Fig. 4. Mean effects plot for the Sdr roughness parameter: (a) base, (b) side

Based on the results, insufficient evidence exists to conclude that the selected manufacturing parameters significantly impact the roughness response variable. However, for the roughness parameters Sz and Sdr, it was observed that the scanning speed does influence the surface roughness. In contrast, none of the selected parameters affected the roughness response variable for Sa and Vmc. This model had a standard deviation of 70.3%.

4.2 Difference obtained between the side and the base of the piece.

This investigation evaluated six surface roughness parameters commonly used to describe surface topography in terms of peaks, valleys, and smoothness, as defined by ISO 25178 [44]. These parameters were selected to identify the most effective manufacturing parameters in reducing surface roughness.

Analyzing the results presented in Fig 2, Fig 3, Fig 4, it can be concluded that the manufacturing parameters of laser power and scanning speed do not exert the same influence on all surface roughness parameters. Specifically, for the base of the specimens, the scanning speed significantly affects the Sa and Vmc parameters, while it has no significant impact on the Sz and Sdr parameters.

On the other hand, the scanning speed significantly affects all the evaluated roughness parameters for the side of the cylinder, indicating a consistent relationship between this manufacturing parameter and surface roughness. In contrast, the laser power does not significantly impact the parameters in this region. These findings suggest that the choice of manufacturing parameters influences surface roughness differently depending on the specific region of the piece being analyzed.

Table 6 shows the nomenclature used in the comparison of means used to compare the final surface roughness obtained on each combination of manufacturing parameters.

Fig 5 shows the plot compares treatments (combinations of parameters) with the roughness Sa obtained. It highlights that a specific set of manufacturing parameters designed to reduce surface roughness Sa on the side of the piece may result in higher surface roughness on the base of the piece. It can be observed that reducing the surface roughness on the base of the pieces manufactured by SLM requires an increase in scanning speed. However, increasing the scanning speed simultaneously increases the surface roughness on the side of the same piece and vice versa.This phenomenon can be attributed to the inherent nature of the SLM process.

Similar findings have been reported by Elsayed et al., Rezaei et al., Yan et al., and Özel et al. [35, 45, 46, 47] in their respective investigations. The SLM process is influenced by various thermodynamic effects that vary depending on the specific part of the manufactured piece. For the base of the piece, surface roughness is primarily affected by the laser strategy, as this area is more susceptible to the markings left by the laser [48].

Additionally, it has been observed that when the laser power is high and the scanning speed is low, the surface tension within the molten pool increases. This causes portions of the melted material to detach from the pool and migrate to other surface areas due to the Marangoni effect, thus exacerbating the balling effect on the surface [28, 49]. The phenomenon described above also occurs on the sides of the piece: “layer border.” However, due to the remelting process during the manufacture of each layer, the balling effect created is remelted on the surface, thereby reducing its impact on the layer border [9, 50].

Conversely, the layer border undergoes a distinct physical effect that alters the surfaces in this area. This effect is attributed to the reheating process that occurs during the layer-by-layer process of SLM. As a result, the grains of the material undergo a recrystallization process, leading to the formation of grains with different sizes and shapes depending on the laser power and scanning speed parameters. Specifically, when both the scanning speed and laser power are high, the temperature and cooling rates increase, giving rise to a specific type of grain known as equiaxial grains. [46, 51].

The grains formed during this process exhibit a specific orientation known as columnar dendrites, which leads to waviness on the side of the pieces. Additionally, the Marangoni effect in this process results in the formation of small balling on the surface, referred to as debris [28, 29].

Fig 6 shows the columnar dendrites observed in one of the specimens manufactured using SLM.

Fig 7 shows the differences in the obtained surfaces. On the base of the piece, the primary defects affecting surface roughness are the laser track and the balling caused by the Marangoni effect. On the side, particularly at the "layer border," waviness caused by the columnar dendrites and a distinct surface pattern resulting from the remelting process can be observed.

For the Selective Laser Melting technique, it is impossible to reduce surface roughness uniformly across the entire piece in a single process. In this case, it is recommended to apply manufacturing parameters that yield a similar roughness across the whole piece. This approach ensures a more homogeneous surface, which is beneficial for subsequent surface finishing during post-processing [52, 53].

Table 5. Nomenclature used to compare surface roughness in Figure 3-4

	Set of parameters	Part of the piece	Sa (µm)
A1	500 mm/s - 75 W	Base	45.57
A2	500 mm/s - 75 W	Side	6.37
B1	500 mm/s – 125 W	Base	22.79
B2	500 mm/s – 125 W	Side	4.01
C1	600 mm/s – 75 W	Base	36.88
C2	600 mm/s – 75 W	Side	8.99
D1	600 mm/s – 125 W	Base	21.77
D2	600 mm/s – 125 W	Side	7.87
E1	700 mm/s – 75 W	Base	24.38
E2	700 mm/s – 75W	Side	9.82
F1	700 mm/s – 125 W	Base	13.62
F2	700 mm/s – 125 W	Side	10.17
G1	800 mm/s – 75 W	Base	16.03
G2	800 mm/s – 75 W	Side	10.14
H1	800 mm/s – 125 W	Base	22.19
H2	800 mm/s – 125 W	Side	9.10

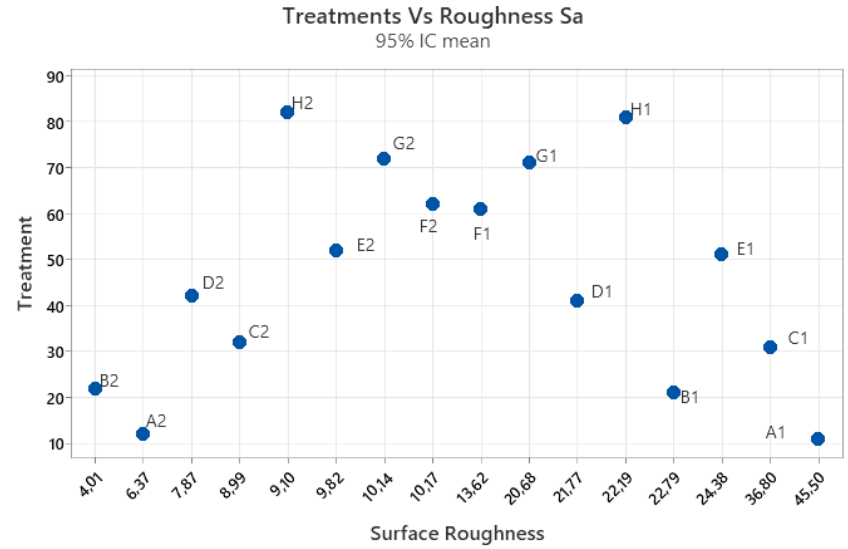

Individual standard deviations were used to calculate the intervals.

Fig. 5. Surface roughness comparison at the side and base of the piece

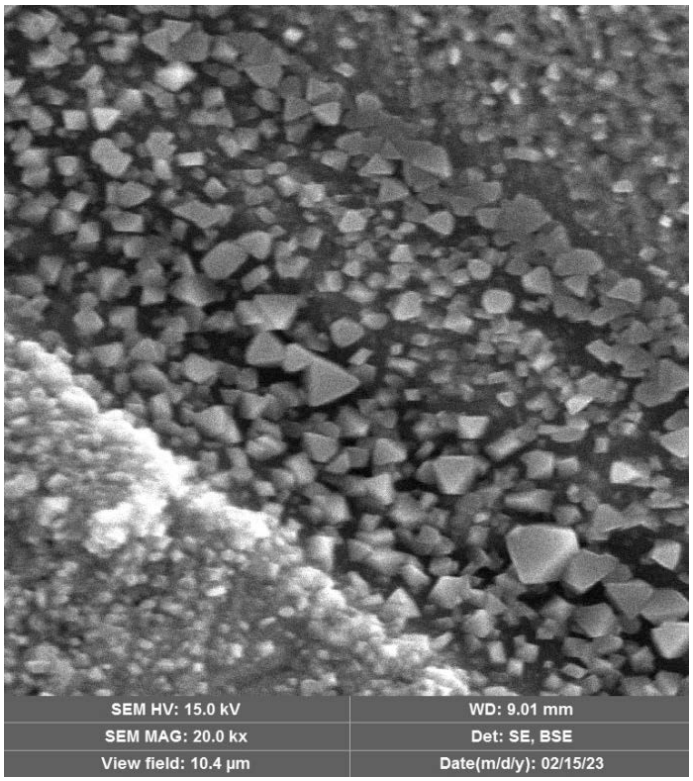

Fig. 6. Dendrites present on the material manufactured with a scan speed of 600 mm/s and 100 W

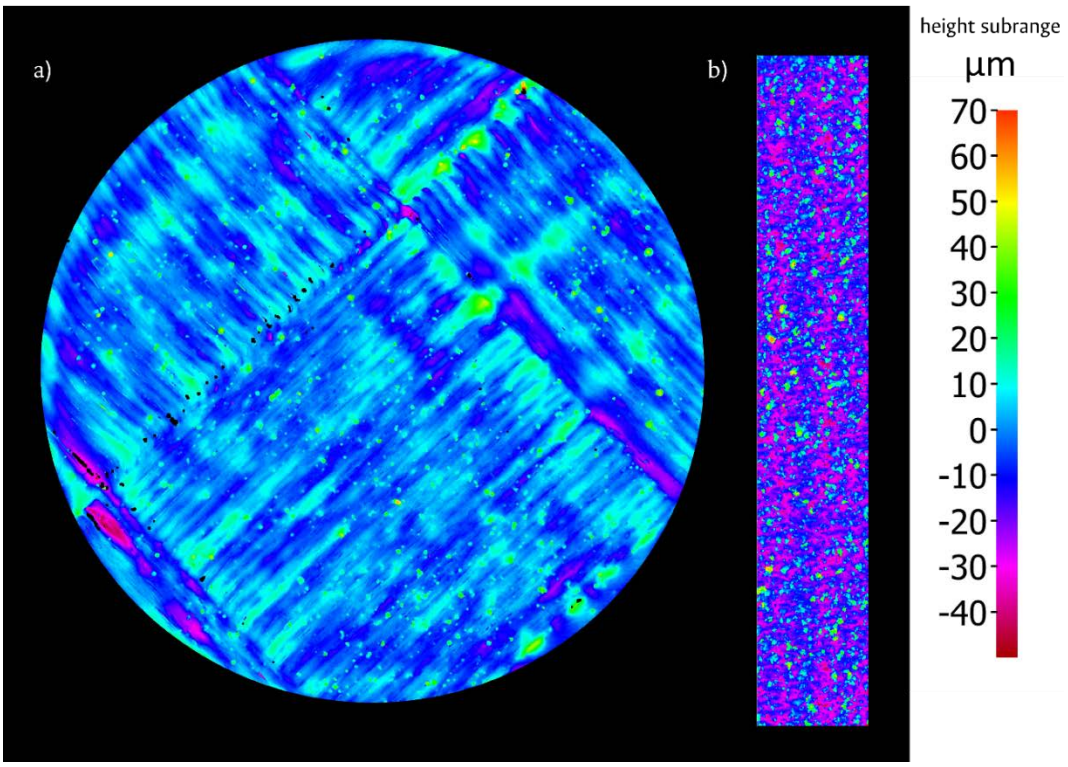

Fig. 7. Differences between the a) base of the cylinder and b) side “Layer border” of the cylinder c) height profile on the base d) height profile on the side

5 CONCLUSIONS

From this investigation, it can be concluded that no single set of manufacturing parameters for the Selective Laser Melting process can uniformly reduce the final surface roughness across all surfaces of a piece. The inherent nature of the process causes variations in surface roughness in different parts of the same piece. Furthermore, efforts to reduce roughness in one area using specific parameters may inadvertently increase roughness in another area, highlighting the region-dependent influence of manufacturing parameters on surface roughness.

The study also demonstrates that different manufacturing parameters have distinct effects on the analyzed roughness parameters. Based on these findings, it is recommended to use a set of manufacturing parameters that result in consistent or homogeneous roughness across all piece surfaces. Following this, surface finishing post-processing can be applied to reduce surface roughness further. This approach is essential for achieving a uniform surface roughness after post-processing, as the initial roughness significantly influences the final roughness following surface finishing.

6 ACKNOWLEDGMENT

The authors would like to thank the Universidad Nacional de Colombia, the GIBM research group, and the Colombian Ministry of Sciences Minciencias for their funding through the Bicentennial Doctoral Excellence Scholarships program.

7 REFERENCES

[1] M. G. & R. B. Stéphane Gorsse, Christopher Hutchinson, “Additive manufacturing of metals_ a brief review of the characteristic microstructures and properties,” Sci Technol Adv Mater, vol. 18, no. 1, p. 29, 2017, doi: 10.1080/14686996.2017.1361305.

[2] J. J. Lewandowski and M. Seifi, “Metal Additive Manufacturing: A Review of Mechanical Properties,” Apr. 16, 2016, Case Western Reserve University, Cleveland. doi: 10.1146/annurev-matsci-070115-032024.

[3] D. Gu, Laser additive manufacturing of high-performance materials. 2015. doi: 10.1007/978-3-662-46089-4.

[4] “Selective Laser Melting,” 2020. doi: 10.3390/books978-3-03928-579-2.

[5] C. Y. Yap et al., “Review of selective laser melting: Materials and applications,” Appl Phys Rev, vol. 2, no. 4, 2015, doi: 10.1063/1.4935926.

[6] Y. Lu et al., “CoCrWCu alloy with antibacterial activity fabricated by selective laser melting: Densification, mechanical properties and microstructural analysis,” 2017, doi: 10.1016/j.powtec.2017.11.018.

[7] Y. S. Song Bo, Shifeng Wen, Chunze Yan, Qingsong Wei, Selective Laser Melting for Metal and Metal Matrix Composites -. Elsevier, 2020. Accessed: May 31, 2021. [Online]. Available:

https://books.google.com.co/books?id=rOneDwAAQBAJ&printsec=frontcover&dq=selective+laser+melting&hl=es&sa=X&redir_esc=y#v=onepage&q=selective laser melting&f=false

[8] F. E. Wiria, S. L. Sing, and W. Y. Yeong, Selective laser melting of novel titanium-tantalum alloy as orthopedic biomaterial. 2020.

[9] I. Yadroitsev, P. Krakhmalev, and I. Yadroitsava, “Hierarchical design principles of selective laser melting for high quality metallic objects,” Addit Manuf, vol. 7, no. 1, pp. 45–56, Dec. 2015, doi: 10.1016/j.addma.2014.12.007.

[10] Y. Wei et al., “Micro selective laser melting of SS316L: Single Tracks, Defects, microstructures and Thermal/Mechanical properties,” Opt Laser Technol, vol. 145, no. 1, pp. 107469–107481, Aug. 2022, doi: 10.1016/j.optlastec.2021.107469.

[11] B. Zhang, Y. Li, and Q. Bai, “Defect Formation Mechanisms in Selective Laser Melting: A Review,” Chinese Journal of Mechanical Engineering (English Edition), vol. 30, no. 3, pp. 515–527, Apr. 2017, doi: 10.1007/s10033-017-0121-5.

[12] S. Afkhami, M. Dabiri, S. H. Alavi, T. Björk, and A. Salminen, “Fatigue characteristics of steels manufactured by selective laser melting,” Int J Fatigue, vol. 122, no. November 2018, pp. 72–83, 2019, doi: 10.1016/j.ijfatigue.2018.12.029.

[13] J. J. Babu, M. Mehrpouya, T. C. Pijper, G. Willemsen, and T. Vaneker, “An Experimental Study of Downfacing Surfaces in Selective Laser Melting,” Adv Eng Mater, vol. 24, no. 8, pp. 1–11, 2022, doi: 10.1002/adem.202101562.

[14] S. Leuders et al., “On the mechanical behaviour of titanium alloy TiAl6V4 manufactured by selective laser melting: Fatigue resistance and crack growth performance,” Int J Fatigue, vol. 48, pp. 300–307, 2013, doi: 10.1016/j.ijfatigue.2012.11.011.

[15] E. Ossola, A. A. Shapiro, A. Pate, S. Firdosy, E. Brusa, and R. Sesana, “Fabrication defects and limitations of AlSi10Mg lattice structures manufactured by selective laser melting,” https://doi-org.ezproxy.unal.edu.co/10.1177/14644207211012726, vol. 235, no. 9, pp. 2071–2082, Apr. 2021, doi: 10.1177/14644207211012726.

[16] A. K. Singla et al., “Selective laser melting of Ti6Al4V alloy: Process parameters, defects and post-treatments,” J Manuf Process, vol. 64, no. 1, pp. 161–187, Jan. 2021, doi: 10.1016/j.jmapro.2021.01.009.

[17] Z.-C. Fang, Z.-L. Wu, C.-G. Huang, and C.-W. Wu, “Review on residual stress in selective laser melting additive manufacturing of alloy parts,” Opt Laser Technol, vol. 129, no. 1, pp. 106283–106298, Dec. 2020, doi: 10.1016/j.optlastec.2020.106283.

[18] F. Simoni, A. Huxol, and F. J. Villmer, “Improving surface quality in selective laser melting based tool making,” 2021. doi: 10.1007/s10845-021-01744-9.

[19] R. K. Enneti, R. Morgan, and S. V Atre, “Effect of process parameters on the Selective Laser Melting (SLM) of tungsten,” International journal of refractory metals y hard materials, vol. 71, no. 1, pp. 315–319, Dec. 2017, doi: 10.1016/j.ijrmhm.2017.11.035.

[20] H. S. Park, D. S. Nguyen, T. Le-Hong, and X. Van Tran, “Machine learning-based optimization of process parameters in selective laser melting for biomedical applications,” J Intell Manuf, vol. 33, no. 6, pp. 1843–1858, 2022, doi: 10.1007/s10845-021-01773-4.

[21] J. Li, J. Hu, Y. Zhu, X. Yu, M. Yu, and H. Yang, “Surface roughness control of root analogue dental implants fabricated using selective laser melting,” Addit Manuf, vol. 34, no. 34, p. 101283, 2020, doi: 10.1016/j.addma.2020.101283.

[22] I. N. Bobrovskij, “How to Select the most Relevant Roughness Parameters of a Surface: Methodology Research Strategy,” in IOP Conference Series: Materials Science and Engineering, Institute of Physics Publishing, Feb. 2018. doi: 10.1088/1757-899X/302/1/012066.

[23] B. Azarhoushang and A. Daneshi, “Workpiece surface roughness,” Tribology and Fundamentals of Abrasive Machining Processes: Third Edition, vol. 1, pp. 575–590, Jan. 2022, doi: 10.1016/B978-0-12-823777-9.00015-X.

[24] P. Champigneux, C. Renault-Sentenac, D. Bourrier, C. Rossi, M.-L. Delia, and A. Bergel, “Effect of surface roughness, porosity and roughened micro-pillar structures on the early formation of microbial anodes,” 2019, doi: 10.1016/j.bioelechem.2019.03.002.

[25] K. Bazaka, R. J. Crawford, and E. P. Ivanova, “Do bacteria differentiate between degrees of nanoscale surface roughness?,” Biotechnol J, vol. 6, no. 9, pp. 1103–1114, 2011, doi: 10.1002/biot.201100027.

[26] Sculpteo, “3D printing: understanding the layer thickness,” Sculpteo. Accessed: Nov. 15, 2022. [Online]. Available: https://www.sculpteo.com/blog/2015/07/29/make-beautiful-3d-prints-understanding-the-layer-thickness/

[27] K. Ökten and A. Biyikoğlu, “Development of thermal model for the determination of SLM process parameters,” Opt Laser Technol, vol. 137, no. October 2020, 2021, doi: 10.1016/j.optlastec.2020.106825.

[28] M. Boutaous, X. Liu, D. A. Siginer, and S. Xin, “Balling phenomenon in metallic laser based 3D printing process,” International Journal of Thermal Sciences, vol. 167, no. 1, pp. 107011–1070211, Sep. 2021, doi: 10.1016/j.ijthermalsci.2021.107011.

[29] R. Tadmor, “Marangoni flow revisited,” J Colloid Interface Sci, vol. 332, no. 1, pp. 451–454, Dec. 2009, doi: 10.1016/j.jcis.2008.12.047.

[30] G. Strano, L. Hao, R. M. Everson, and K. E. Evans, “Surface roughness analysis, modelling and prediction in selective laser melting,” J Mater Process Technol, vol. 213, no. 4, pp. 589–597, 2013, doi: 10.1016/j.jmatprotec.2012.11.011.

[31] B. Fotovvati and K. Chou, “Build surface study of single-layer raster scanning in selective laser melting: Surface roughness prediction using deep learning,” Manuf Lett, vol. 33, pp. 701–711, Sep. 2022, doi: 10.1016/j.mfglet.2022.07.088.

[32] E. Maleki, S. Bagherifard, M. Bandini, and M. Guagliano, “Surface post-treatments for metal additive manufacturing: Progress, challenges, and opportunities,” Addit Manuf, vol. 37, no. 1, pp. 101619–101631, May 2021, doi: 10.1016/j.addma.2020.101619.

[33] M. A. Baciu, E. R. Baciu, C. Bejinariu, S. L. Toma, A. Danila, and C. Baciu, “Influence of Selective Laser Melting Processing Parameters of Co-Cr-W Powders on the Roughness of Exterior Surfaces,” IOP Conf Ser Mater Sci Eng, vol. 374, no. 1, pp. 12010–12016, 2018, doi: 10.1088/1757-899X/374/1/012010.

[34] S. Milton, A. Morandeau, F. Chalon, and R. Leroy, “Influence of Finish Machining on the Surface Integrity of Ti6Al4V Produced by Selective Laser Melting,” Procedia CIRP, vol. 45, pp. 127–130, 2016, doi: 10.1016/j.procir.2016.02.340.

[35] M. Elsayed, M. Ghazy, Y. Youssef, and K. Essa, “Optimization of SLM Process Parameters for Ti6Al4V Medical Implants,” Birmingham, 2018. doi: 10.1108/RPJ-05-2018-0112.

[36] Sisma/mysint100, “MYSINT100, Laser Metal Fusion metal 3D printing technology,” www.sisma.com/en/products/mysint100. Accessed: Feb. 01, 2023. [Online]. Available: https://www.sisma.com/en/products/mysint100/

[37] Scheftner.dental, “Starbond Easy Powder 30 - Scheftner Dental Alloys,” Sheftmer.dental/starbond. Accessed: Mar. 07, 2023. [Online]. Available: https://scheftner.dental/starbond-easy-powder-30-en.html

[38] Universidad Nacional de Colombia - Sede Bogotá, “Laboratorio de Metrología Dimensional de Precisión - Universidad Nacional de Colombia.” Accessed: Jun. 08, 2023. [Online]. Available: https://ingenieria.unal.edu.co/metrodim/

[39] Alicona, “Alicona ' s Optical Roughness Measurement,” Pocket Poster, pp. 1–12, 2015, [Online]. Available: https://www.alicona.com/publications/publication/bruker-aliconas-optical-roughness-measurement/

[40] Minitab, “Diseños ortogonales de Taguchi fraccionados,” support minitab. [Online]. Available: https://support.minitab.com/es-mx/minitab/21/help-and-how-to/statistical-modeling/doe/supporting-topics/taguchi-designs/dummy-treatments-for-taguchi-designs/

[41] C. J. Cortés-Rodríguez, F. C. Herreño Cuestas, and I. Z. Areque-Salazar, Medición de Rugosidad Superficial 3D, 1st ed., vol. 1. Kassel: Kassel University press, 2019.

[42] J. J. Lifton and T. Liu, “Evaluation of the standard measurement uncertainty due to the ISO50 surface determination method for dimensional computed tomography,” Precis Eng, vol. 61, pp. 82–92, 2020, doi: 10.1016/j.precisioneng.2019.10.004.

[43] W. Grzesik, “Prediction of the Functional Performance of Machined Components Based on Surface Topography: State of the Art,” J Mater Eng Perform, vol. 25, no. 10, pp. 4460–4468, 2016, doi: 10.1007/s11665-016-2293-z.

[44] International Standard, “ISO 25178-606.,” Switzerland, Jun. 2015.

[45] A. Rezaei et al., “Microstructural and mechanical anisotropy of selective laser melted IN718 superalloy at room and high temperatures using small punch test,” Mater Charact, vol. 162, no. 1, pp. 110200–110213, Feb. 2020, doi: 10.1016/j.matchar.2020.110200.

[46] X. Yan et al., “Effect of building directions on the surface roughness, microstructure, and tribological properties of selective laser melted Inconel 625,” Journal of materials processing tech., vol. 288, no. 1, pp. 116878–116889, Aug. 2020, doi: 10.1016/j.jmatprotec.2020.116878.

[47] T. Özel, A. Altay, B. Kaftanoglu, R. Leach, N. Senin, and A. Donmez, “Focus variation measurement and prediction of surface texture parameters using machine learning in laser powder bed fusion,” Journal of Manufacturing Science and Engineering, Transactions of the ASME, vol. 142, no. 1, Jan. 2020, doi: 10.1115/1.4045415.

[48] Y. Du, T. Mukherjee, and T. DebRoy, “Physics-informed machine learning and mechanistic modeling of additive manufacturing to reduce defects,” Appl Mater Today, vol. 24, no. 1, pp. 101123–101135, Sep. 2021, doi: 10.1016/j.apmt.2021.101123.

[49] Marcello Lappa, “Numerical Techniques and Insights into Physics,” in Fluids, Materials and Microgravity, First., vol. 1, Elsevier Science 2004, 2004, ch. 3, pp. 1–538.

[50] I. Yadroitsev and I. Smurov, “Selective laser melting technology: From the single laser melted track stability to 3D parts of complex shape,” in Physics Procedia, Elsevier B.V., 2010, pp. 551–560. doi: 10.1016/j.phpro.2010.08.083.

[51] X. Zhou et al., “Textures formed in a CoCrMo alloy by selective laser melting,” J Alloys Compd, vol. 631, no. 1, pp. 153–164, Jan. 2015, doi: 10.1016/j.jallcom.2015.01.096.

[52] Y. Kaynak, O. Kitay, and E. Tascioglu, “Post-processing effects on the surface characteristics of Inconel 718 alloy fabricated by selective laser melting additive manufacturing,” Addit Manuf, vol. 26, no. September 2018, pp. 221–234, 2019, doi: 10.1007/s40964-019-00099-1.

[53] Y. Kaynak and O. Kitay, “The effect of post-processing operations on surface characteristics of 316L stainless steel produced by selective laser melting,” Addit Manuf, vol. 26, no. September 2018, pp. 84–93, 2019, doi: 10.1016/j.addma.2018.12.021.

Paper submitted: 21.07.2023.

Paper accepted: 22.11.2024.